Pergamon

*Int. J. Solids Structures* Vol. 35, No. 23, pp. 3097–3103, 1998

0020–7683/98 $19.00 + .00

**PII: S0020–7683(97)00358–2**

# ON THE BALLISTIC RESISTANCE OF MULTI-LAYERED TARGETS WITH AIR GAPS

G. BEN-DOR, A. DUBINSKY and T. ELPERIN*
Pearlstone Center for Aeronautical Engineering, Department of Mechanical Engineering, Ben-Gurion University of the Negev, P.O. Box 653, Beer-Sheva, 84105, Israel

(*Received* 21 *May* 1997; *in revised form* 11 *November* 1997)

**Abstract**—High velocity penetration of a 3-D rigid sharp impactor into a ductile layered target with air gaps between the plates is studied using the assumption about the localized projectile–target interaction. The special property of the penetration phenomenon for conical-nosed impactors is established, namely, that the ballistic performance of the target is independent on the air gap widths and on the sequence of the plates in the target. Similar results are also obtained for 3-D non-conical impactors on the basis of some class of models. These findings are in good agreement with available experimental results. © 1998 Elsevier Science Ltd. All rights reserved.

## 1. INTRODUCTION

The review of investigations on sub-ordnance penetration and perforation of multi-layered plates can be found in the recent study by Corbett *et al.* (1996). The important subject of the theoretical and the experimental investigations in this field is the comparison between the resistance properties of targets with the same total thickness, depending on the layering, the sequence of the plates in the target, and the widths of the air gaps between the layers (Almohandes *et al.*, 1996; Ben-Dor *et al.*, 1997b; Corran *et al.*, 1983; Marom and Bodner, 1978; Radin and Goldsmith, 1988). Since a rigorous theory is not feasible at present, simple analytical models are used (Marom and Bodner, 1978; Radin and Goldsmith, 1988). These simple analytical models allow one to establish the qualitative laws which can be used as the basis for further theoretical and experimental investigations. Similar approach employing the projectile–target interaction models and the equation of motion of the impactor in the target rather than the integral balance relation is applied in this study to investigate the influence of the air gaps and the sequence of the plates in the target on its ballistic resistance.

A high speed normal penetration of a rigid sharp striker into a ductile target with a finite thickness with air gaps is considered. The basic notations are shown in Fig. 1a. The coordinate $h$, the depth of penetration, is defined as the distance between the nose of the impactor and the upper surface of the target. The coordinate $\xi$ is associated with the target. We assume that the shape of the 3-D impactor is such that the total force is directed along the $h$-axis. The cylindrical coordinates $x$, $r$, $\theta$ are associated with the impactor, and its surface is described by the following equation:

$$r = \Phi(x, \theta), \quad 0 \leqslant x \leqslant L, \quad 0 \leqslant \theta \leqslant 2\pi \tag{1}$$

where $L$ is the length of the impactor. Assume that the target consists of $N$ plates with the thicknesses $b_1, b_2, b_3, \ldots, b_N$ where the $i$-th plate is located between the sections $\xi = \xi_i$ and $\xi = \xi_i + b_i$, $\xi_1 = 0$, $i = 1, 2, \ldots, N$ and the total thickness of the target is $b = \xi_N + b_N$. The part of the lateral surface of the impactor between the cross-sections $x = x_1$ and $x = x_2$ (see Fig. 1a) interacts with some layers of the target or is in contact with some air gaps where (see Fig. 1b)

* Author to whom correspondence should be addressed. Fax: 00972 76472813. E-mail: elperin@menix.bgu.ac.il.

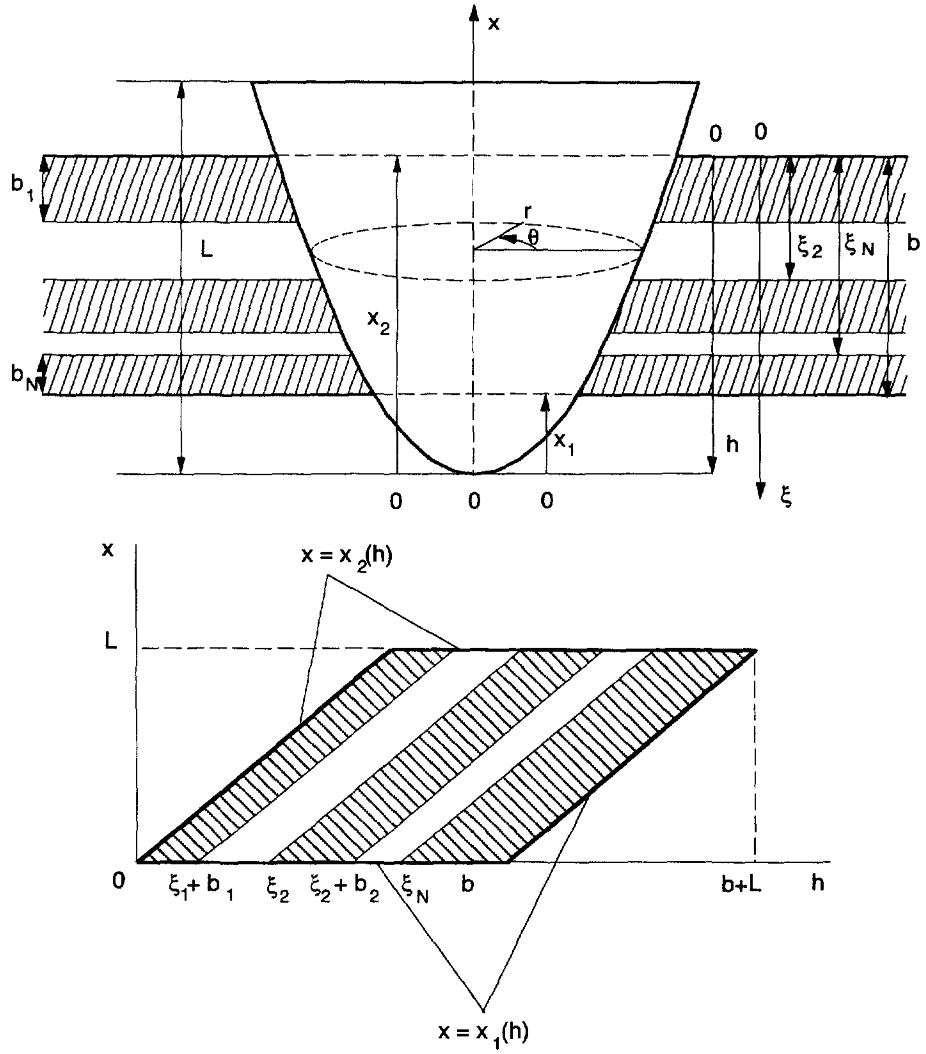


Fig. 1a, b. Coordinates and notations.

$$x_1(h)=\begin{cases}0 & \text{if } 0\leqslant h\leqslant b\\ h-b & \text{if } b\leqslant h\leqslant b+L\end{cases},\quad x_2(h)=\begin{cases}h & \text{if } 0\leqslant h\leqslant L\\ L & \text{if } b\leqslant h\leqslant b+L\end{cases}. \tag{2}$$

The equation of motion of the impactor $M\,\mathrm{d}^2h/\mathrm{d}t^2=-D$ can be rewritten as follows:

$$Mv\frac{\mathrm{d}v}{\mathrm{d}h}=-D \tag{3}$$

where the instantaneous velocity of the impactor $v$ is considered to be a function of $h$, $M$ is the mass of the impactor, and $D$ is the resistance force. We consider the range of impact velocities $v_s$ when the projectile perforates the target. The position of the striker at the moment of perforation is $h=b+L$ and its residual velocity is $v_r$. The ballistic limit velocity $v_*$ is defined as the impact velocity of the impactor required to emerge from the target with a zero residual velocity.

## 2. 3-D CONICAL IMPACTORS

In this section we assume that the material of all the layers of the target is the same and that the impactor–target interaction at a given location at the surface of the impactor which is in contact with the target can be represented using localized interaction model (Ben-Dor *et al.*, 1997a, 1998; Bunimovich and Dubinsky, 1995), i.e.,

$$\mathrm{d}\mathbf{F} = (\Omega_n \mathbf{n}^0 + \Omega_\tau \boldsymbol{\tau}^0)\,\mathrm{d}S \tag{4}$$

where

$$\boldsymbol{\tau}^0 = -\frac{\mathbf{v}^0 + u\mathbf{n}^0}{\sqrt{1-u^2}}, \quad u = \cos\beta = -\mathbf{v}^0 \cdot \mathbf{n}^0. \tag{5}$$

In eqns (4) and (5), $\mathrm{d}\mathbf{F}$ is the force acting at the surface element $\mathrm{d}S$ of the impactor, $\mathbf{n}^0$ and $\boldsymbol{\tau}^0$ are the unit normal and tangent vectors at a given location on the impactor's surface, respectively, $\mathbf{v}^0$ is the unit vector of the impactor's velocity, $\beta$ is the angle between $\mathbf{n}^0$ and $-\mathbf{v}^0$. The non-negative functions $\Omega_n = \Omega_n(a_1, a_2, \ldots; u, v)$ and $\Omega_\tau = \Omega_\tau(a_1, a_2, \ldots; u, v)$ determine the specific model ($\Omega_n = \Omega_\tau = 0$ if $u \leqslant 0$). The parameters $a_\nu$ depend on the properties of the material of the target, hereafter they are not listed, in order to simplify notations, in the list of arguments. Equations (4) and (5) comprise most if not all of the known phenomenological models for homogenous targets. Their description and analysis can be found, e.g., in the studies of Backman and Goldsmith (1978), Goldsmith (1960), Landgrov and Sarkisyan (1984), Recht (1990), Vitman and Stepanov (1959). In the present study the detailed specification of the model is not required.

The total force $\mathbf{F}$ is determined by integrating the local force over the impactor–target contact surface $\sigma$ taking into account the air gaps. Using formulae of differential geometry

$$u = A/B, \quad A = \Phi\Phi_x, \quad B = \sqrt{\Phi^2(\Phi_x^2+1)+\Phi_\theta^2}, \quad \mathrm{d}S = B\,\mathrm{d}x\,\mathrm{d}\theta, \tag{6}$$

where the subscript denotes a derivative with respect to the corresponding variable, the expression for the drag force $D$ can be written as

$$D = \mathbf{F}\cdot(-\mathbf{v}^0) = \iint_\sigma u\Omega_0(u,v)\,\mathrm{d}S = \int_{x_1(h)}^{x_2(h)} \int_0^{2\pi} \delta(h-x)\Omega_0(u,v)A\,\mathrm{d}x\,\mathrm{d}\theta \tag{7}$$

where

$$\Omega_0(u,v) = \Omega_n(u,v) + u^{-1}\sqrt{1-u^2}\,\Omega_\tau(u,v) \tag{8}$$

and $\delta(\xi) = 1$ if $\xi_i \leqslant \xi \leqslant \xi_i + b_i$ for $1 \leqslant i \leqslant N$ and $\xi = 0$ otherwise.

For a 3-D conical impactor, $\Phi(x,\theta) = x\eta(\theta)$ where the function $\eta(\theta)$ determines its cross-sectional contor and $\eta(0) = \eta(2\pi)$. Then, after substituting the expressions

$$u = u_0(\theta) = \frac{\eta\eta_\theta}{\sqrt{\eta^4+\eta^2+\eta_\theta^2}}, \quad A = x\eta^2 \tag{9}$$

to eqn (7), eqn (3) can be written as follows:

$$Mv\frac{\mathrm{d}v}{\mathrm{d}h} = -\omega(v)\int_{x_1(h)}^{x_2(h)} x\delta(h-x)\,\mathrm{d}x \tag{10}$$

where

$$\omega(v) = \int_0^{2\pi} \eta^2 \Omega_0(u_0(\theta), v)\, \mathrm{d}\theta \geqslant 0. \tag{11}$$

The solution of eqn (10) with the initial condition $v(0) = v_s$ which corresponds to the beginning of the motion of the impactor with an impact velocity $v_s$ reads

$$\varphi(v_s) - \varphi(v) = \frac{\chi(h)}{M} \tag{12}$$

where the increasing function $\varphi(v)$ and the function $\chi(h)$ are determined by the following formulae:

$$\varphi(v) = \int_0^v \frac{z\,\mathrm{d}z}{\omega(z)}, \quad \chi(h) = \int_0^h \mathrm{d}\tilde{h} \int_{x_1(\tilde{h})}^{x_2(\tilde{h})} x\delta(\tilde{h}-x)\,\mathrm{d}x. \tag{13}$$

Equation (12) yields formulae for the residual velocity $v_r = v(b+L)$ and the ballistic limit velocity $v_*$:

$$\varphi(v_s) - \varphi(v_r) = a, \quad v_* = \varphi^{-1}(a) \tag{14}$$

where

$$a = \frac{\chi(b+L)}{M}. \tag{15}$$

Since (see Fig. 1b)

$$\chi(b+L) = \int_0^{b+L} \mathrm{d}\tilde{h} \int_{x_1(\tilde{h})}^{x_2(\tilde{h})} x\delta(\tilde{h}-x)\,\mathrm{d}x = \int_0^L x\,\mathrm{d}x \int_x^{x+b} \delta(\tilde{h}-x)\,\mathrm{d}\tilde{h}$$

$$= \int_0^L x\,\mathrm{d}x \sum_{i=1}^N \int_{\xi_i}^{\xi_i+b} \mathrm{d}\xi = \frac{L^2}{2}\sum_{i=1}^N b_i \tag{16}$$

we find that

$$a = \frac{L^2}{2M} b_\Sigma, \quad b_\Sigma = \sum_{i=1}^N b_i. \tag{17}$$

Formally, eqn (17) shows that the residual velocity for a given impact velocity and the ballistic limit velocity are the same for all targets with the same total thickness $b_\Sigma$. However, our model does not account for the difference in the resistance properties of a monolithic target and a target consisting of several plates in-contact with the same total thickness which is found in the experiments (e.g., Almohandes *et al.*, 1996; Marom and Bodner, 1978; Radin and Goldsmith, 1988). In this study we consider targets which consist of some given set of plates and analyze only the effect of the air gap's widths and of the sequence of the plates in the target on its ballistic properties. Thus, the above results can be interpreted as an independence of these properties on air gaps widths and on the sequence of the plates.

## 3. NON-CONICAL 3-D IMPACTORS

We assume now that the resistance force $\mathrm{d}D_i$ acting on the impactor element inside the $i$-th plate between sections $x$ and $x+\mathrm{d}x$ can be represented as follows:

$$\mathrm{d}D_i = G_i(h-\xi_i, x)\omega(v)\,\mathrm{d}x, \quad \xi_i \leqslant h-x \leqslant \xi_i+b_i \tag{18}$$

where $G_i$ and $\omega$ are the functions determining the impactor–plate interaction model, the first function depends on the shape of the impactor and the properties of the material of the plate as well. Equation (18) can be written also in the following generally accepted form:

$$\mathrm{d}D_i = \tilde{G}_i(h-\xi_i, x)\omega(v)\,\mathrm{d}s, \quad \tilde{G}_i = \frac{G}{\int_0^{2\pi} \Phi\Phi_\theta\,\mathrm{d}\theta} \tag{19}$$

where d$s$ is the elementary "presented area" (e.g., Recht, 1990), i.e., the projection of the contact surface between sections $x$ and $x+\mathrm{d}x$ on a plane normal to the impactor's velocity. Unlike the model given by eqns (4) and (5), the model of eqn (18) does not specify the character of the interaction of the impactor with the target at every point of its contact. It allows to account for the differences in the models used for different plates and specifies the relation between the resistance force an the velocity of the impactor.

In the following we present several examples of the models used for a monolithic target and which can be reduced to the model determined by eqn (18), or, equivalently, to the model given by eqn (19).

The first example is the set of phenomenological models (Backman and Goldsmith, 1978; Goldsmith, 1960) with $\tilde{G} = 1$, $\omega(v) = a^{(2)}v^{(2)}+a^{(1)}v+a^{(0)}$ where the parameters $a^{(0)}$, $a^{(1)}$, $a^{(2)}$ depend on the shape of the impactor and the properties of the material of the target which are assumed to be the same for all the plates. If the velocity of the impactor is low, the model with $\tilde{G}_i = a_i^{(2)}$ and $\omega(v) = v^2$ is used. As the second example, we consider the model based on the relation $F = kv^p$ between the penetration resistance $F$ and the impactor's velocity $v$ which was suggested and studied by Mileiko and Sarkisyan (1980), Mileiko *et al.* (1994), Muzychenko and Postnov (1984) where the parameter $p$ depends, primarily, on the properties of the target material and the parameter $k$ depends also on the shape of the impactor. The latter model yields generally wrong non-zero values of resistance at the beginning and at the end of the penetration with a non-zero velocity. Therefore, it is more appropriate to use it for the cross-section of the impactor in the form given by eqn (18) with $\omega(v) = v^p$.

The equation of motion of the impactor reads:

$$Mv\frac{\mathrm{d}v}{\mathrm{d}h} = -\omega(v)\int_{x_1(h)}^{x_2(h)} G(h,x)\delta(h-x)\,\mathrm{d}x \tag{20}$$

where $G = G_i(h-\xi_i, x)$ if $\xi_i \leqslant h-x \leqslant \xi_i+b_i$ and $G = 0$ otherwise. The solution of this equation with the initial condition $v(0) = v_s$ is given by eqn (12) where the function $\varphi$ is determined by eqn (13), whereas

$$\chi(h) = \int_0^h \mathrm{d}\tilde{h}\int_{x_1(\tilde{h})}^{x_2(\tilde{h})} G(\tilde{h},x)\delta(\tilde{h}-x)\,\mathrm{d}x. \tag{21}$$

After transformations we obtain eqns (14) and (15) where

$$\chi(b+L) = \int_0^L \mathrm{d}x\int_x^{x+b} G(\tilde{h},x)\delta(\tilde{h}-x)\,\mathrm{d}\tilde{h} = \int_0^L \mathrm{d}x\sum_{i=1}^N\int_{\xi_i}^{\xi_i+b} G_i(h-\xi_i,x)\,\mathrm{d}\xi$$

$$= \sum_{i=1}^N\int_0^L \mathrm{d}x\int_0^{b_i} G_i(\mu,x)\,\mathrm{d}\mu \tag{22}$$

i.e., the residual velocity for a given impact velocity and the ballistic limit velocity are independent of the air gap's widths and of the sequence of the plates in the target.

## 4. DISCUSSION

Experimental data on ballistic penetration of conical impactors into ductile targets with air gaps are quite scarce. In a study by Radin and Goldsmith (1988), the impact response of a hard-steel 60-grad conical-nosed projectile on a target with multi-layered plates of soft aluminum was investigated. Two experiments are relevant to our study. In the first experiment, two plates with thicknesses 1.6 mm, both adjacent and space, are considered, and the ballistic limit velocities of 93.2 m/s and 90.6 m/s were obtained, respectively. In the second experiment, the plates with thicknesses 3.2 mm are used; the ballistic limit velocities 160.4 m/s and 153.4 m/s were obtained, respectively. The values of ballistic limits for adjacent and spaced plates are close; some increase in the ballistic limit of plates in contact therewith can be explained by friction between the layers (Corran *et al.*, 1983) which is not taken into account in the present models.

Consider now the non-conical projectiles. It is known (Recht, 1990) that a ballistic resistance of a sharp impactor is weakly affected by the shape of its longitudinal contor at high impact velocities. It was even found (Zukas, 1982) that ogive-shaped noses could be replaced in the calculations by equivalent conical ones. Therefore, one would have expected that the above proved assertion for cones is approximately valid with the same accuracy for non-conical sharp impactors, despite the fact that it is determined in Section 2 using less reliable models. This conclusion is supported by the experimental results by Almohandes *et al.* (1996) where the standard 7.62 mm bullet with 8 mm core diameter and a slenderness ratio of 4.2 mm was used. The total thickness of the mild steel plates was 8 mm. We divide the results of the experiments into several groups (see Table 1). In every group, the target consists of some set of the plates which are arranged in different experiments in different sequences, both adjacent and space. We use the notation of Almohandes *et al.* (1996): 2S–6A–6S for the targets that comprises, sequentially, of 2 mm steel plate, 6 mm air gap, and 6 mm steel plate; the notation 4*(1S–6A) denotes 1S–6A–1S–6A–1S–6A–1S–6A, etc. In Table 1, the average value $\bar{v}_r$ and the deviations $\varepsilon$ are calculated using the following formulas:

$$\bar{v}_r = \frac{1}{m}\sum_{i=1}^{N} v_r^{(i)}, \quad \varepsilon = \frac{1}{\bar{v}_r}\sqrt{\frac{1}{m}\sum_{i=1}^{N}(v_r^{(i)} - \bar{v}_r)^2} \tag{23}$$

where $m$ is the number of variants of the target in the group, $v_r^{(1)}$ is the residual velocity in

Table 1. Effect of the target configuration on the residual velocity (on the basis of experiments by Almohandes, 1996)

| Target configurations | Parameter | Impact velocity (m/s) 706.0 | 754.5 | 775.4 | 804.5 | 862.2 |
|---|---|---|---|---|---|---|
| 2S–6S, 6S–2S, | Average $\bar{v}_r$, m/s | 475.0 | 520.2 | 548.1 | 613.0 | 657.9 |
| 2S–6A–6S, 6S–6A–2S | Average deviation $\varepsilon$, % | 0.5 | 0.7 | 0.5 | 0.4 | 0.7 |
| 4S–4S, | Average $\bar{v}_r$, m/s | 487.2 | 564.7 | 534.2 | 643.7 | 668.1 |
| 4S–6A–4S | Average deviation $\varepsilon$, % | 0.2 | 0.2 | 0.4 | 0.1 | 0.1 |
| 1S–6A–1S–6A–6S, | Average $\bar{v}_r$, m/s | 479.8 | 524.2 | 551.0 | 641.0 | 665.7 |
| 6S–6A–1S–6A–1S | Average deviation $\varepsilon$, % | 0.9 | 2.7 | 2.6 | 0.5 | 0.3 |
| 2S–6A–2S–6A–4S, | Average $\bar{v}_r$, m/s | 493.8 | 540.5 | 579.3 | 649.2 | 676.6 |
| 4S–6A–2S–6A–2S | Average deviation $\varepsilon$, % | 0.2 | 0.3 | 0.1 | 0.9 | 0.4 |
| 4*(1S–6A)–4S, | Average $\bar{v}_r$, m/s | 523.1 | 563.2 | 610.9 | 657.0 | 679.6 |
| 4S–4*(6A–1S) | Average deviation $\varepsilon$, % | 0.8 | 1.8 | 0.4 | 0.5 | 0.6 |
| All targets | Average $\bar{v}_r$, m/s | 489.0 | 533.7 | 568.7 | 636.1 | 667.6 |
| | Average deviation $\varepsilon$, % | 3.5 | 3.2 | 4.2 | 2.7 | 1.4 |

the experiment for a given variant of target configuration and a given impact velocity. The group "all target" includes all the considered variants of the target configuration. Table 1 shows that the residual velocities for different targets of every group are very close; the difference becomes negligible if the plates in contact are not included (Almohandes *et al.*, 1996). In the group "all targets", the scatter in the residual velocities is more noticeable.

## 5. CONCLUDING REMARKS

The main result of our investigation is that the ballistic performance of the ductile layered target penetrated by 3-D rigid, sharp, conical-nosed impactors is independent of the air gap widths between the layers and on the sequence of the plates in the target. The latter results is proved using a quite general model that describes the projectile–target interaction. Similar results have also been obtained for 3-D non-conical impactors using some class of models for a projectile–target interaction. The obtained results are found to be in a good agreement with available experimental data.

## REFERENCES

Almohandes, A. A., Abdel-Kader, M. S. and Eleiche, A. M. (1996) Experimental investigation of the ballistic resistance of steel–fiberglass reinforced polyester laminated plates. *Composites* **27B**, 447–458.

Backman, M. E. and Goldsmith, W. (1978) The mechanics of penetration of projectiles into targets. *International Journal of Engineering Science* **16**(1), 1–99.

Ben-Dor, G., Dubinsky, A. and Elperin, T. (1997a) Area rules for penetrating bodies. *Theoretical and Applied Fracture Mechanics* **26**, 193–198.

Ben-Dor, G., Dubinsky, A. and Elperin, T. (1997b) Optimal 3D impactors penetrating into layered targets. *Theoretical and Applied Mechanics* **27**, 161–166.

Ben-Dor, G., Dubinsky, A. and Elperin, T. (1998) New area rule for penetrating impactors. *International Journal of Impact Engineering* **21**(1–2), 51–59.

Bunimovich, A. I. and Dubinsky, A. V. (1995) *Mathematical Models and Methods of Localized Interaction Theory*. World Sci. Publ.

Corbett, G. G., Reid, S. R. and Jonson, W. (1996) Impact loading of plates and shells by free-flying projectiles: a review. *International Journal of Impact Engineering* **18**(2), 141–230.

Corran, R. S. J., Shadbolt, P. J. and Ruiz, C. (1983) Impact loading of plates—an experimental investigation. *International Journal of Impact Engineering* **1**(1), 3–22.

Goldsmith, W. (1960) *Impact. The Theory and Physical Behavior of Colliding Solids*. Edward Arnold, London.

Landgrov, I. F. and Sarkisyan, O. A. (1984) Piercing plastic-material barriers with a rigid punch. *J. Appl. Mech. Tech. Phys.* No. 5, 771–773.

Marom, I. and Bodner, S. R. (1978) Projectile perforation of multi-layered beams. *Int. J. Mech. Sci.* **21**, 489–504.

Mileiko, S. T. and Sarkisyan, O. A. (1980) Phenomenological model of punch-through. *J. Appl. Mech. Tech. Phys.* No. 5, 711–713.

Mileiko, S. T., Sarkisyan, O. A. and Kondakov, S. F. (1994) Ballistic limits of Al-6% Mg allow laminated by diffusion bonding. *Theoretical and Applied Fracture Mechanics* **21**, 9–16.

Muzychenko, V. P. and Postnov, V. I. (1984) Scope for forecasting allow piercing resistance, No. 5, 774–776.

Radin, J. and Goldsmith, W. (1988) Normal projectile penetration and perforation of layered targets. *International Journal of Impact Engineering* **7**(2), 229–259.

Recht, R. F. (1990) High velocity impact dynamics: analytical modeling of plate penetration dynamics. In *High Velocity Impact Dynamics*, ed. J. A. Zukas, Chap. 7. Wiley Interscience Publ., New York.

Vitman, F. F. and Stepanov, V. A. (1959) Effect of the strain rate on the resistance of metals to deformation at impact velocities 100–1000 m/s. In *Nekotoryje Problemy Prochnosti Tverdogo Tela*, Academy of Science of the Soviet Union, Moscow, Leningrad, pp. 207–221, in Russian.

Zukas, J. A. (1982) Penetration and perforation of solids. In *Impact Dynamics*, ed. J. A. Zukas, T. Nicholas, H. F. Swift, L. B. Greszczuk and D. R. Curran, Chap. 5, pp. 155–214. John Wiley and Sons, New York.